

INFLUENCE OF THE IN-PLANE BOUNDARY CONDITIONS ON THE NATURAL FREQUENCY OF CYLINDRICALLY CURVED PANELS WITH SIMPLY SUPPORTED EDGES

YUJI MATSUZAKI†

National Aerospace Laboratory, Tokyo, Japan

Abstract—The natural frequency of roof-shaped panels is evaluated on the basis of Reissner's simplified equations for thin shallow shells, which are approximately solved with the aid of Galerkin's method. The flexural vibration mode is assumed in a form of Fourier series and a homogeneous solution of stress function is expressed in terms of trigonometric and hyperbolic functions in order to satisfy several sets of the in-plane boundary conditions exactly. The modal equations are generally coupled and hence every natural mode is a general combination of the assumed modes. Numerical results in two-mode approximation indicate that the conditions at straight edges are more influential than the conditions at curved edges for a panel of $\lambda \gtrsim 1$, where λ is defined as the ratio of the length of straight edges to that of curved edges. In particular, the restriction on the normal displacement at straight edges raises the natural frequency of the lower frequency mode to a great extent. For $\lambda \lesssim 1$ the conditions at curved edges are very influential. At curved edges the condition of zero tangential displacement gives more restrictions to a panel of $\lambda < 1.83$ rather than that of zero normal displacement. As for the higher frequency mode the influence of the in-plane boundary conditions is diminished.

NOTATION

a	a half of length of a panel along straight edges
b	a half of breadth of projection of a panel on x - y plane (see Fig. 1)
D	$Eh^3/12(1-\nu^2)$
E	Young's modulus
F	stress function
h	thickness of panel
N_x, N_y, N_{xy}	stress resultants
$I(m, n)$	see equation (23)
$J_{oo}(m, n)$, etc.	see equations (24)
R	radius of curvature
u, v, w	displacements in x, y and z directions, respectively
w_{mn}	modal amplitude
\bar{w}_{mn}	see equation (21)
x, y, z	coordinates
$Z(x, y)$	geometry of panel
$\alpha_m, \beta_m, \gamma_n, \delta_n$	see equations (12)
$\alpha_m^*, \beta_m^*, \gamma_n^*, \delta_n^*$	see equations (19)
λ	aspect ratio = a/b
ν	Poisson's ratio
ρ_m	density of panel
Δ	$\partial^2/\partial x^2 + \partial^2/\partial y^2$
ω	natural frequency
Ω	dimensionless natural frequency, see equation (22)
(p, q)	a natural mode predominated by p and q half-waves in x and y directions, respectively

† Research Engineer, First Airframe Division.

1. INTRODUCTION

THE analysis of flexural vibration of curved panels is essential to aeroelastic and acoustic problems of high-speed aircrafts and rockets in which curved panels are fundamental structural components.

For curved panels with simply supported edges early works based on a modal approach were performed by Vlasov [1], Palmer [2] and Reissner [3]. Palmer gave the frequency formula of clamped edge panels, too. Reissner derived the simplified equations from the shallow shell theory of Marguerre [4] by omitting the effect of in-plane inertia on a basis of an order-of-magnitude analysis. Kobayashi [5] gave the natural frequency of simply supported edge panels constrained by the condition that zero normal displacement at the edges was satisfied on an average and showed the occurrence of coupling of the assumed modes. Sewall [6] presented the frequency equations of curved panels with simply supported or clamped edges by employing the beam vibration mode and compared theoretical results with available experimental data. Webster [7] calculated the natural frequency for clamped panels approximating the vibration mode by truncated double-power series and evaluated a range of panel geometry for which Sewall's equations gave accurate results. For two-dimensional curved panels Dowell [8] indicated the coupling behavior of the assumed modes in a symmetrical form.

It can be concluded from the results of the above-mentioned investigations that natural frequency of curved panels is greatly affected by both curvature and edge conditions. As for the analysis of vibration of cylindrical shells, Forsberg [9] solved numerically the eighth-order characteristic equation and indicated that the in-plane boundary conditions have a great influence on the natural frequency.

In the present paper the effect of the in-plane boundary conditions on the natural frequency of curved panels with simply supported edges is investigated as well as the effect of panel geometry. Forsberg's method may be applicable to an analysis of curved panels. However, the present investigation is a preliminary one for panel flutter problem of curved panels. It is too laborious to apply the method to the flutter problem.

Recently, the buckling analysis of a fundamental mode of curved panels including the effect of the in-plane boundary conditions on critical loads is presented by Hayashi and Kondo [10] using a modal approach. They have expressed a homogeneous solution of stress function in terms of trigonometric and hyperbolic functions to satisfy the in-plane boundary conditions exactly. Such an approach is taken here by employing Reissner's simplified equations for thin shallow shells.

2. ANALYSIS

The strain-displacement relations of the middle-surface of a thin shallow curved panel are given as

$$\left\{ \begin{array}{l} \varepsilon_{x0} = \frac{\partial u}{\partial x} + \frac{\partial Z}{\partial x} \frac{\partial w}{\partial x} \\ \varepsilon_{y0} = \frac{\partial v}{\partial y} + \frac{\partial Z}{\partial y} \frac{\partial w}{\partial y} \\ \gamma_{xy0} = \frac{\partial u}{\partial y} + \frac{\partial v}{\partial x} + \frac{\partial Z}{\partial x} \frac{\partial w}{\partial y} + \frac{\partial Z}{\partial y} \frac{\partial w}{\partial x} \end{array} \right. \quad (1)$$

where $Z = Z(x, y)$ is the geometry of the middle-surface of the panel and Hooke's law as

$$\begin{cases} \varepsilon_{x0} = (N_x - \nu N_y)/Eh \\ \varepsilon_{y0} = (N_y - \nu N_x)/Eh \\ \gamma_{xy0} = 2(1 + \nu)N_{xy}/Eh. \end{cases} \quad (2)$$

Figure 1 shows the panel geometry defined as

$$Z = \frac{b^2 - y^2}{2R} \quad (3)$$

and coordinate system.

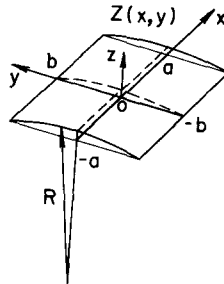


FIG. 1. Rectangular cartesian coordinates and shell geometry.

Reissner's equations of equilibrium and compatibility in the linear theory are given as follows:

$$D\Delta\Delta w - h \frac{\partial^2 F}{\partial y^2} \frac{\partial^2 Z}{\partial x^2} - h \frac{\partial^2 F}{\partial x^2} \frac{\partial^2 Z}{\partial y^2} + 2h \frac{\partial^2 F}{\partial x \partial y} \frac{\partial^2 Z}{\partial x \partial y} + \rho_m h \frac{\partial^2 w}{\partial t^2} = 0 \quad (4)$$

$$\Delta\Delta F = E \left[2 \frac{\partial^2 Z}{\partial x \partial y} \frac{\partial^2 w}{\partial x \partial y} - \frac{\partial^2 Z}{\partial y^2} \frac{\partial^2 w}{\partial x^2} - \frac{\partial^2 Z}{\partial x^2} \frac{\partial^2 w}{\partial y^2} \right] \quad (5)$$

where D , E and F are bending stiffness, Young's modulus and stress function defined as

$$\frac{\partial^2 F}{\partial y^2} = \frac{N_x}{h}, \quad \frac{\partial^2 F}{\partial x^2} = \frac{N_y}{h}, \quad \frac{\partial^2 F}{\partial x \partial y} = -\frac{N_{xy}}{h}. \quad (6)$$

The simply supported edge conditions are taken:

$$w = \partial^2 w / \partial x^2 = 0 \quad \text{at } x = -a \text{ and } a \quad (7.1)$$

$$w = \partial^2 w / \partial y^2 = 0 \quad \text{at } y = -b \text{ and } b. \quad (7.2)$$

The following sets of the in-plane boundary conditions which are the same at the opposite sides of edges are considered :

$$\left\{ \begin{array}{l} S_x1: u = v = 0 \\ \text{or } S_x2: N_x = v = 0 \\ \text{or } S_x3: u = N_{xy} = 0 \\ \text{or } S_x4: N_x = N_{xy} = 0 \quad \text{at } x = -a \text{ and } x = a, \end{array} \right. \tag{8.1}$$

$$\left\{ \begin{array}{l} S_y1: v = u = 0 \\ \text{or } S_y2: N_y = u = 0 \\ \text{or } S_y3: v = N_{xy} = 0 \\ \text{or } S_y4: N_y = N_{xy} = 0 \quad \text{at } y = -b \text{ and } y = b. \end{array} \right. \tag{8.2}$$

In a subsequent section, description of derivation of the modal equations will be divided into four parts corresponding to the vibration mode.

2.1 *Odd numbers of half-waves in x and y directions*

The flexural vibration mode is assumed so as to satisfy equations (7.1) and (7.2) as follows :

$$w = \sum_{\substack{m=1 \\ m,n:\text{ odd}}}^{\infty} \sum_{n=1}^{\infty} w_{mn}(t) \cos \frac{m\pi}{2a} x \cos \frac{n\pi}{2b} y. \tag{9.1}$$

Substitution of equations (9.1) and (3) into equation (5) yields a solution of stress function as

$$F = F_p + F_h \tag{10.1}$$

where F_p and F_h are particular and homogeneous solutions, respectively and

$$F_p = - \sum_m \sum_n \frac{E w_{mn}}{R} \left(\frac{2a}{\pi} \right)^2 \frac{m^2}{(m^2 + n^2 \lambda^2)^2} \cos \frac{m\pi}{2a} x \cos \frac{n\pi}{2b} y \tag{11.1}$$

$$F_h = \frac{E}{R} \left[\sum_m \cos \frac{m\pi}{2a} x \left(\alpha_m \cosh \frac{m\pi}{2a} y + \beta_m \frac{m\pi}{2a} y \sinh \frac{m\pi}{2a} y \right) + \sum_n \cos \frac{n\pi}{2b} y \left(\gamma_n \cosh \frac{n\pi}{2b} x + \delta_n \frac{n\pi}{2b} x \sinh \frac{n\pi}{2b} x \right) \right]. \tag{12.1}$$

Equations (10.1) and (6) yield stress resultants as

$$\begin{aligned} \frac{N_x}{h} = & \frac{E}{R} \left[\sum_m \sum_n w_{mn} \frac{m^2 n^2 \lambda^2}{(m^2 + n^2 \lambda^2)^2} \cos \frac{m\pi}{2a} x \cos \frac{n\pi}{2b} y \right. \\ & + \sum_m \left(\frac{m\pi}{2a} \right)^2 \cos \frac{m\pi}{2a} x \left\{ (\alpha_m + 2\beta_m) \cosh \frac{m\pi}{2a} y + \beta_m \frac{m\pi}{2a} y \sinh \frac{m\pi}{2a} y \right\} \\ & \left. - \sum_n \left(\frac{n\pi}{2b} \right)^2 \cos \frac{n\pi}{2b} y \left(\gamma_n \cosh \frac{n\pi}{2b} x + \delta_n \frac{n\pi}{2b} x \sinh \frac{n\pi}{2b} x \right) \right] \tag{13.1} \end{aligned}$$

$$\begin{aligned} \frac{N_y}{h} = & \frac{E}{R} \left[\sum_m \sum_n w_{mn} \frac{m^4}{(m^2 + n^2 \lambda^2)^2} \cos \frac{m\pi}{2a} x \cos \frac{n\pi}{2b} y \right. \\ & - \sum_m \left(\frac{m\pi}{2a} \right)^2 \cos \frac{m\pi}{2a} x \left(\alpha_m \cosh \frac{m\pi}{2a} y + \beta_m \frac{m\pi}{2a} y \sinh \frac{m\pi}{2a} y \right) \\ & \left. + \sum_n \left(\frac{n\pi}{2b} \right)^2 \cos \frac{n\pi}{2b} y \left\{ (\gamma_n + 2\delta_n) \cosh \frac{n\pi}{2b} x + \delta_n \frac{n\pi}{2b} x \sinh \frac{n\pi}{2b} x \right\} \right] \end{aligned} \quad (14.1)$$

$$\begin{aligned} \frac{N_{xy}}{h} = & \frac{E}{R} \left[\sum_m \sum_n w_{mn} \frac{\lambda m^3 n}{(m^2 + n^2 \lambda^2)^2} \sin \frac{m\pi}{2a} x \sin \frac{n\pi}{2b} y \right. \\ & + \sum_m \left(\frac{m\pi}{2a} \right)^2 \sin \frac{m\pi}{2a} x \left\{ (\alpha_m + \beta_m) \sinh \frac{m\pi}{2a} y + \beta_m \frac{m\pi}{2a} y \cosh \frac{m\pi}{2a} y \right\} \\ & \left. + \sum_n \left(\frac{n\pi}{2b} \right)^2 \sin \frac{n\pi}{2b} y \left\{ (\gamma_n + \delta_n) \sinh \frac{n\pi}{2b} x + \delta_n \frac{n\pi}{2b} x \cosh \frac{n\pi}{2b} x \right\} \right]. \end{aligned} \quad (15.1)$$

The displacements u and v are derived from equations (1), (2) and (10.1) as

$$\begin{aligned} u(x) = & \int_0^x \frac{\partial u}{\partial x} dx = \int_0^x \frac{1}{Eh} (N_x - \nu N_y) dx \\ = & \frac{1}{R} \left[\sum_m \sum_n w_{mn} \frac{2a}{\pi} \frac{m(n^2 \lambda^2 - \nu m^2)}{(m^2 + n^2 \lambda^2)^2} \sin \frac{m\pi}{2a} x \cos \frac{n\pi}{2b} y \right. \\ & + \sum_m \frac{m\pi}{2a} \sin \frac{m\pi}{2a} x \left\{ (\alpha_m + \nu \alpha_m + 2\beta_m) \cosh \frac{m\pi}{2a} y + \beta_m (1 + \nu) \frac{m\pi}{2a} y \sinh \frac{m\pi}{2a} y \right\} \\ & - \sum_n \frac{n\pi}{2b} \cos \frac{n\pi}{2b} y \left\{ (\gamma_n + \nu \gamma_n + 2\nu \delta_n) \sinh \frac{n\pi}{2b} x \right. \\ & \left. + \delta_n (1 + \nu) \left(\frac{n\pi}{2b} x \cosh \frac{n\pi}{2b} x - \sinh \frac{n\pi}{2b} x \right) \right\} \right], \end{aligned} \quad (16.1)$$

$$\begin{aligned} v(y) = & \int_0^y \frac{\partial v}{\partial y} dy = \int_0^y \left\{ \frac{1}{Eh} (N_y - \nu N_x) - \frac{\partial Z}{\partial y} \frac{\partial w}{\partial y} \right\} dy \\ = & \frac{1}{R} \left[- \sum_m \sum_n w_{mn} \frac{2a}{\pi} \frac{\lambda n \{ \lambda^2 n^2 + (2 + \lambda) m^2 \}}{(m^2 + n^2 \lambda^2)^2} \cos \frac{m\pi}{2a} x \sin \frac{n\pi}{2b} y \right. \\ & + \sum_m \sum_n w_{mn} y \cos \frac{m\pi}{2a} x \cos \frac{n\pi}{2b} y \\ & - \sum_m \frac{m\pi}{2a} \cos \frac{m\pi}{2a} x \left\{ (\alpha_m + \nu \alpha_m + 2\nu \beta_m) \sinh \frac{m\pi}{2a} y \right. \\ & \left. + \beta_m (1 + \nu) \left(\frac{m\pi}{2a} y \cosh \frac{m\pi}{2a} y - \sinh \frac{m\pi}{2a} y \right) \right\} \\ & \left. + \sum_n \frac{n\pi}{2b} \sin \frac{n\pi}{2b} y \left\{ (\gamma_n + \nu \gamma_n + 2\delta_n) \cosh \frac{n\pi}{2b} x + \delta_n (1 + \nu) \frac{n\pi}{2b} x \sinh \frac{n\pi}{2b} x \right\} \right]. \end{aligned} \quad (17.1)$$

Since, for this vibration mode, the displacements are symmetric with respect to the $x = 0$ and $y = 0$ sections, the conditions $u = 0$ and $v = 0$ are satisfied at $x = 0$ and $y = 0$, respectively. By means of equations (13.1)–(17.1) each in-plane boundary condition leads to the equations with respect to the unknown quantities $\alpha_m, \beta_m, \gamma_n$ and δ_n ($m = 1, 3, 5, \dots$ and $n = 1, 3, 5, \dots$) as

$x = -a$ and a ;

$$u = 0: \quad \alpha_m = \beta_m = 0 \tag{OOX-1}$$

$$\begin{aligned} & \gamma_n(1 + \nu) \sinh \frac{n\pi}{2} \lambda + \delta_n \left\{ (1 + \nu) \frac{n\pi}{2} \lambda \cosh \frac{n\pi}{2} \lambda - (1 - \nu) \sinh \frac{n\pi}{2} \lambda \right\} \\ & = \sum_{\substack{r=1 \\ r: \text{odd}}}^{\infty} \left(\frac{2a}{\pi} \right)^2 \frac{r(\lambda^2 n^2 - \nu r^2)}{\lambda n(r^2 + n^2 \lambda^2)^2} w_{rn} \sin \frac{r\pi}{2} \end{aligned} \tag{OOX-2}$$

$$v = 0: \quad \alpha_m \text{ and } \beta_m \text{ are arbitrary.} \tag{OOX-3}$$

$$\gamma_n(1 + \nu) \cosh \frac{n\pi}{2} \lambda + \delta_n \left\{ (1 + \nu) \frac{n\pi}{2} \lambda \sinh \frac{n\pi}{2} \lambda + 2 \cosh \frac{n\pi}{2} \lambda \right\} = 0 \tag{OOX-4}$$

$$N_x = 0: \quad \text{equation (OOX-3)}$$

$$\gamma_n \cosh \frac{n\pi}{2} \lambda + \delta_n \frac{n\pi}{2} \lambda \sinh \frac{n\pi}{2} \lambda = 0 \tag{OOX-5}$$

$$N_{xy} = 0: \quad \text{equation (OOX-1)}$$

$$\gamma_n \sinh \frac{n\pi}{2} \lambda + \delta_n \left(\sinh \frac{n\pi}{2} \lambda + \frac{n\pi}{2} \lambda \cosh \frac{n\pi}{2} \lambda \right) = - \sum_{\substack{r=1 \\ r: \text{odd}}}^{\infty} \left(\frac{2a}{\pi} \right)^2 \frac{r^3}{\lambda n(r^2 + n^2 \lambda^2)^2} w_{rn} \sin \frac{r\pi}{2} \tag{OOX-6}$$

$y = -b$ and b ;

$$v = 0: \quad \gamma_n = \delta_n = 0 \tag{OOY-1}$$

$$\begin{aligned} & \alpha_m(1 + \nu) \sinh \frac{m\pi}{2\lambda} + \beta_m \left\{ (1 + \nu) \frac{m\pi}{2\lambda} \cosh \frac{m\pi}{2\lambda} - (1 - \nu) \sinh \frac{m\pi}{2\lambda} \right\} \\ & = - \sum_{\substack{s=1 \\ s: \text{odd}}}^{\infty} \left(\frac{2a}{\pi} \right)^2 \frac{\lambda s \{ s^2 \lambda^2 + (2 + \nu) m^2 \}}{m(m^2 + s^2 \lambda^2)^2} w_{ms} \sin \frac{s\pi}{2} \end{aligned} \tag{OOY-2}$$

$$u = 0: \quad \gamma_n \text{ and } \delta_n \text{ are arbitrary.} \tag{OOY-3}$$

$$\alpha_m(1 + \nu) \cosh \frac{m\pi}{2\lambda} + \beta_m \left\{ (1 + \nu) \frac{m\pi}{2\lambda} \sinh \frac{m\pi}{2\lambda} + 2 \cosh \frac{m\pi}{2\lambda} \right\} = 0 \tag{OOY-4}$$

$$N_y = 0: \quad \text{equation (OOY-3)}$$

$$\alpha_m \cosh \frac{m\pi}{2\lambda} + \beta_m \frac{m\pi}{2\lambda} \sinh \frac{m\pi}{2\lambda} = 0 \tag{OOY-5}$$

$$N_{xy} = 0: \quad \text{equation (OOY-1)}$$

$$\alpha_m \sinh \frac{m\pi}{2\lambda} + \beta_m \left(\sinh \frac{m\pi}{2\lambda} + \frac{m\pi}{2\lambda} \cosh \frac{m\pi}{2\lambda} \right) = - \sum_{\substack{s=1 \\ s: \text{odd}}}^{\infty} \left(\frac{2a}{\pi} \right)^2 \frac{\lambda m s}{(m^2 + s^2 \lambda^2)^2} w_{ms} \sin \frac{s\pi}{2} \tag{OOY-6}$$

where

$$\lambda = a/b. \tag{18}$$

Corresponding to the combination of the sets of the in-plane boundary conditions, unknown quantities α_m s, β_m s, γ_n s and δ_n s are easily determined from equations (OOX-1)–(OOX-6) and equations (OOY-1)–(OOY-6) in the general form as

$$\begin{aligned} \alpha_m &= \sum_s \alpha_s^* w_{ms} \\ \beta_m &= \sum_s \beta_s^* w_{ms} \\ \gamma_n &= \sum_r \gamma_r^* w_{rn} \\ \delta_n &= \sum_r \delta_r^* w_{rn} \end{aligned} \tag{19.1}$$

where α_s^* s, β_s^* s, γ_r^* s and δ_r^* s are constants.

The following seven combinations of sets of the in-plane boundary conditions can be derived from equations (OOX-1)–(OOX-6) and equations (OOY-1)–(OOY-6):

- $S_x1: S_y2$
- $S_x2: S_y1, S_y2, S_y3, S_y4$
- $S_x3: S_y2$
- $S_x4: S_y2.$

It is noted that α_s^* s and β_s^* s (or γ_r^* s and δ_r^* s) in equations (19.1) vanish for the case of the set S_y2 (or S_x2).

Finally, equations (9.1), (10.1) and (3) are substituted into the left-hand side of equation (4) and the Galerkin method is used to obtain a coupled set of modal equations:

$$\{I(m, n) - \Omega^2\} \bar{w}_{mn} + J_{oo}(m, n) = 0 \quad (m = 1, 3, 5, \dots \quad n = 1, 3, 5, \dots) \tag{20.1}$$

where

$$w_{mn}(t) = \bar{w}_{mn} \exp(i\omega t) \tag{21}$$

$$\Omega = \omega \left\{ \left(\frac{\pi}{2a} \right)^2 \sqrt{\left(\frac{D}{\rho_m h} \right)} \right\} \tag{22}$$

$$I(m, n) = (m^2 + n^2 \lambda^2)^2 + \frac{12(1 - \nu^2)}{h^2 R^2} \left(\frac{2a}{\pi} \right)^4 \frac{m^4}{(m^2 + n^2 \lambda^2)^2} \tag{23}$$

$$\begin{aligned} J_{oo}(m, n) &= -\frac{24(1 - \nu^2)}{abh^2 R^2} \left(\frac{2a}{\pi} \right)^4 \frac{\lambda mn}{m^2 + n^2 \lambda^2} \\ &\times \left[\frac{m\pi}{2} \sin \frac{n\pi}{2} \left\{ \cosh \frac{m\pi}{2\lambda} \sum_s \alpha_s^* \bar{w}_{ms} + \left(\frac{m\pi}{2\lambda} \sinh \frac{m\pi}{2\lambda} - \frac{2m^2 \cosh(m\pi/2\lambda)}{m^2 + n^2 \lambda^2} \right) \sum_s \beta_s^* \bar{w}_{ms} \right\} \right. \\ &- \frac{n\pi}{2} \sin \frac{m\pi}{2} \left\{ \cosh \frac{n\pi}{2} \lambda \sum_r \gamma_r^* \bar{w}_{rn} \right. \\ &\left. \left. + \left(\frac{n\pi}{2} \lambda \sinh \frac{n\pi}{2} \lambda + \frac{2m^2 \cosh(n\pi/2)\lambda}{m^2 + n^2 \lambda^2} \right) \sum_r \delta_r^* \bar{w}_{rn} \right\} \right]. \end{aligned} \tag{24.1}$$

A characteristic equation is derived as

$$\Lambda = 0 \tag{25}$$

where Λ represents a determinant of the coefficients with respect to the modal amplitudes in equations (20.1). The dimensionless natural frequency Ω is easily obtained from equation (25). Since the assumed modes are generally coupled in the modal equations, each natural mode is a general combination of the assumed modes.

2.2 *Odd and even numbers of half-waves in x and y directions, respectively*

The vibration mode is assumed to be in the form of

$$w = \sum_{\substack{m=1 \\ m: \text{odd}}}^{\infty} \sum_{\substack{n=2 \\ n: \text{even}}}^{\infty} w_{mn}(t) \cos \frac{m\pi}{2a} x \sin \frac{n\pi}{2b} y. \tag{9.2}$$

The stress function is obtained from equations (9.2) and (5) as

$$\begin{aligned} F = \frac{E}{R} & \left[- \sum_m \sum_n w_{mn} \left(\frac{2a}{\pi} \right)^2 \frac{m^2}{(m^2 + n^2 \lambda^2)^2} \cos \frac{m\pi}{2a} x \sin \frac{n\pi}{2b} y \right. \\ & + \sum_m \cos \frac{m\pi}{2a} x \left(\alpha_m \sinh \frac{m\pi}{2a} y + \beta_m \frac{m\pi}{2a} y \cosh \frac{m\pi}{2a} y \right) \\ & \left. + \sum_n \sin \frac{n\pi}{2b} y \left(\gamma_n \cosh \frac{n\pi}{2b} x + \delta_n \frac{n\pi}{2b} x \sinh \frac{n\pi}{2b} x \right) \right]. \tag{10.2} \end{aligned}$$

Since the in-plane condition $N_y = 0$ is identically satisfied by means of equation (10.2) at $y = 0$, the condition $v = 0$ is not satisfied at $x = -a$ and a . Hence, the set $S_{y,1}$ or $S_{y,3}$ is not considered for this vibration mode.

According to the in-plane boundary conditions, the equations with respect to $\alpha_m, \beta_m, \gamma_n$ and δ_n ($m = 1, 3, 5, \dots$ and $n = 2, 4, 6, \dots$) are obtained as $x = -a$ and a ;

$$u = 0: \quad \alpha_m = \beta_m = 0 \tag{OEX-1}$$

$$\begin{aligned} & \gamma_n(1 + \nu) \sinh \frac{n\pi}{2} \lambda + \delta_n \left\{ (1 + \nu) \frac{n\pi}{2} \lambda \cosh \frac{n\pi}{2} \lambda - (1 - \nu) \sinh \frac{n\pi}{2} \lambda \right\} \\ & = \sum_{\substack{r=1 \\ r: \text{odd}}}^{\infty} \left(\frac{2a}{\pi} \right)^2 \frac{r(\lambda^2 n^2 - \nu r^2)}{\lambda n(r^2 + n^2 \lambda^2)^2} w_{rn} \sin \frac{r\pi}{2} \end{aligned} \tag{OEX-2}$$

$$v = 0: \quad \alpha_m \text{ and } \beta_m \text{ are arbitrary.} \tag{OEX-3}$$

$$\gamma_n(1 + \nu) \cosh \frac{n\pi}{2} \lambda + \delta_n \left\{ (1 + \nu) \frac{n\pi}{2} \lambda \sinh \frac{n\pi}{2} \lambda + 2 \cosh \frac{n\pi}{2} \lambda \right\} = 0 \tag{OEX-4}$$

$$N_x = 0: \quad \text{equation (OEX-3)}$$

$$\gamma_n \cosh \frac{n\pi}{2} \lambda + \delta_n \frac{n\pi}{2} \lambda \sinh \frac{n\pi}{2} \lambda = 0 \tag{OEX-5}$$

$N_{xy} = 0:$

equation (OEX-1)

$$\begin{aligned} & \gamma_n \sinh \frac{n\pi}{2} \lambda + \delta_n \left(\sinh \frac{n\pi}{2} \lambda + \frac{n\pi}{2} \lambda \cosh \frac{n\pi}{2} \lambda \right) \\ &= - \sum_{\substack{r=1 \\ r: \text{dd}}}^{\infty} \left(\frac{2a}{\pi} \right)^2 \frac{r^3}{\lambda n (r^2 + n^2 \lambda^2)^2} w_{rn} \sin \frac{r\pi}{2} \end{aligned} \quad (\text{OEX-6})$$

$y = -b$ and $b;$

$u = 0:$

γ_n and δ_n are arbitrary. (OEY-3)

$$\alpha_m (1 + \nu) \sinh \frac{m\pi}{2\lambda} + \beta_m \left\{ (1 + \nu) \frac{m\pi}{2\lambda} \cosh \frac{m\pi}{2\lambda} + 2 \sinh \frac{m\pi}{2\lambda} \right\} = 0 \quad (\text{OEY-4})$$

$N_y = 0:$

equation (OEY-3)

$$\alpha_m \sinh \frac{m\pi}{2\lambda} + \beta_m \frac{m\pi}{2\lambda} \cosh \frac{m\pi}{2\lambda} = 0 \quad (\text{OEY-5})$$

$N_{xy} = 0:$

$\gamma_n = \delta_n = 0$ (OEY-1)

$$\alpha_m \cosh \frac{m\pi}{2\lambda} + \beta_m \left(\cosh \frac{m\pi}{2\lambda} + \frac{m\pi}{2\lambda} \sinh \frac{m\pi}{2\lambda} \right) = \sum_{\substack{s=2 \\ s: \text{even}}}^{\infty} \left(\frac{2a}{\pi} \right)^2 \frac{\lambda m s}{(m^2 + s^2 \lambda^2)^2} w_{ms} \cos \frac{s\pi}{2}. \quad (\text{OEY-6})$$

The following combinations of sets of the in-plane boundary conditions may be chosen :

$S_{x1} : S_{y2}$

$S_{x2} : S_{y2}, S_{y4}$

$S_{x3} : S_{y2}$

$S_{x4} : S_{y2}$

The coupled set of the modal equations is obtained as

$$\{ I(m, n) - \Omega^2 \} \bar{w}_{mn} + J_{oe}(m, n) = 0 \quad (m = 1, 3, 5, \dots \quad n = 2, 4, 6, \dots) \quad (20.2)$$

where

$$\begin{aligned} J_{oe}(m, n) = & - \frac{24(1 - \nu^2)}{abh^2 R^2} \left(\frac{2a}{\pi} \right)^4 \frac{\lambda mn}{m^2 + n^2 \lambda^2} \\ & \times \left[\frac{m\pi}{2} \cos \frac{n\pi}{2} \left\{ \sinh \frac{m\pi}{2\lambda} \sum_s \alpha_s^* \bar{w}_{ms} \right. \right. \\ & + \left. \left. \left(\frac{m\pi}{2\lambda} \cosh \frac{m\pi}{2\lambda} - \frac{2m^2 \sinh(m\pi/2\lambda)}{m^2 + n^2 \lambda^2} \right) \sum_s \beta_s^* \bar{w}_{ms} \right\} \right. \\ & + \frac{n\pi}{2} \sin \frac{m\pi}{2} \left\{ \cosh \frac{n\pi}{2} \lambda \sum_r \gamma_r^* \bar{w}_{rn} \right. \\ & \left. \left. + \left(\frac{n\pi}{2} \lambda \sinh \frac{n\pi}{2} \lambda + \frac{2m^2 \cosh(n\pi/2)\lambda}{m^2 + n^2 \lambda^2} \right) \sum_r \delta_r^* \bar{w}_{rn} \right\} \right]. \quad (24.2) \end{aligned}$$

The dimensionless natural frequency is obtained from the characteristic equation associated with equation (20.2).

Descriptions about the remaining vibration modes will be omitted in the present paper.

3. NUMERICAL RESULTS AND DISCUSSIONS

In the present analysis the influence of the in-plane boundary conditions at $x = -a$ and a (or at $y = -b$ and b) on the natural frequency can be investigated exclusively with the combination of the set S_y2 at the adjoining edges $y = -b$ and b (or the set S_x2 at $x = -a$ and a). The analysis in the preceding section indicates that each natural mode is generally a combination of the assumed modes. However, as for the case of the set S_y2 the w_{ms} s are uncoupled in equations (20) since the α_s^* s and the β_s^* s in equations (19) vanish. It is also true that the w_{ms} are uncoupled in equations (20) for the case of the set S_x2 . Therefore, for the case of the combination of the sets S_x2 and S_y2 the assumed modes are uncoupled and each assumed mode represents a natural mode. The numerical calculations are presented for symmetrical vibration modes and carried out by employing two-mode approximation ($m = 1$ and 3 for $n = 1$ or $n = 1$ and 3 for $m = 1$) in the right-hand side of equation (9.1).

Figures 2(a), 3(a) and 4(a) illustrate the influence of the in-plane boundary conditions at $x = -a$ and a with the combination of the set S_y2 at $y = -b$ and b . The dimensionless natural frequency Ω for panels of aspect ratio $\lambda = 0.5, 1.0$ and 2.0 are plotted against the geometric parameter $4a^2/Rh$. In the figures the natural frequency of a panel constrained

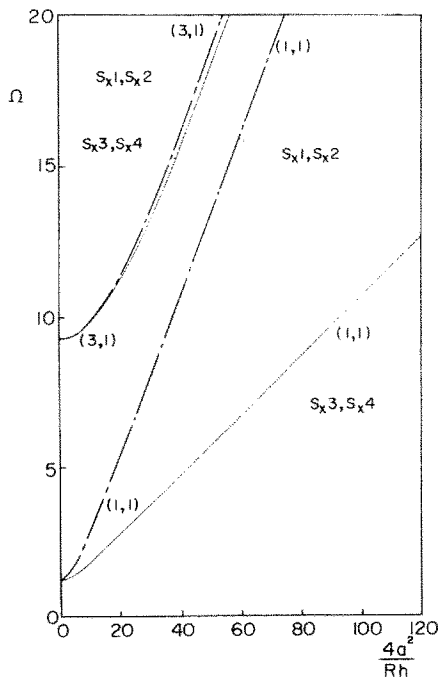


FIG. 2(a). Natural frequencies for $\lambda = 0.5$ with the set S_y2 of the boundary conditions at $y = -b$ and b .

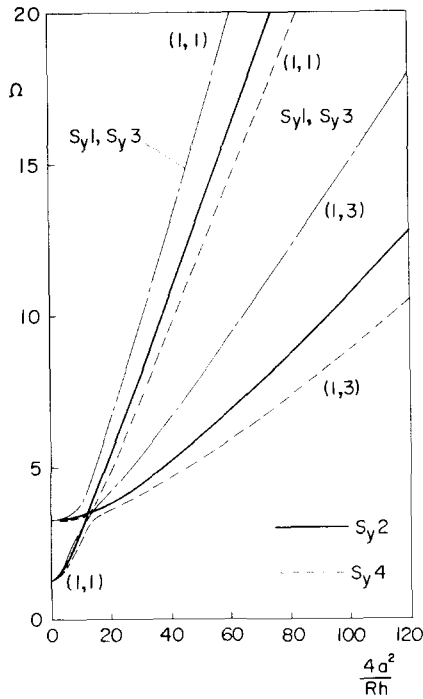


FIG. 2(b). Natural frequencies for $\lambda = 0.5$ with the set S_{x2} of the boundary conditions at $x = -a$ and a .

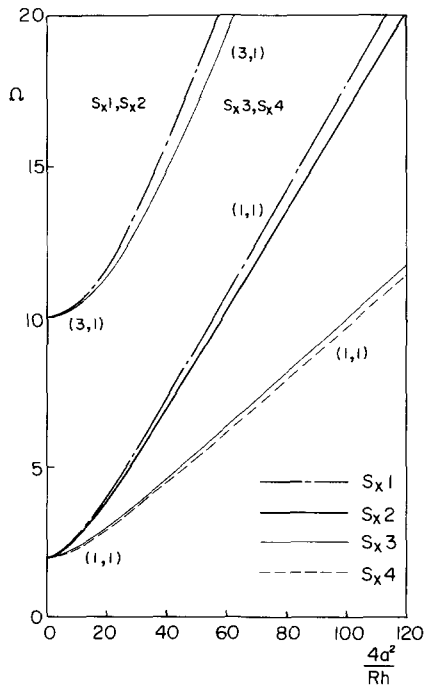


FIG. 3(a). Natural frequencies for $\lambda = 1.0$ with the set S_{y2} of the boundary conditions at $y = -b$ and b .

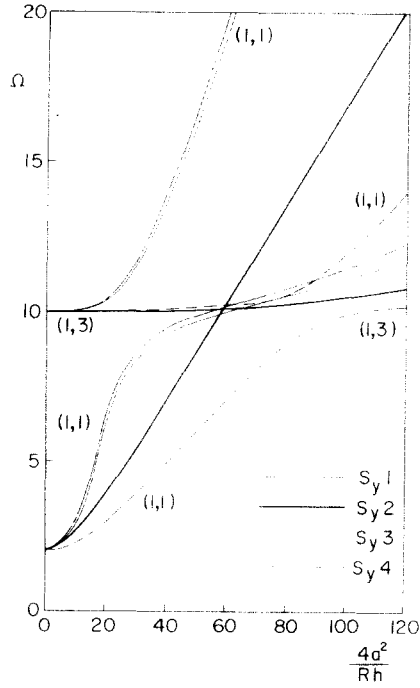


FIG. 3(b). Natural frequencies for $\lambda = 1.0$ with the set $S_{y,2}$ of the boundary conditions at $x = -a$ and a .

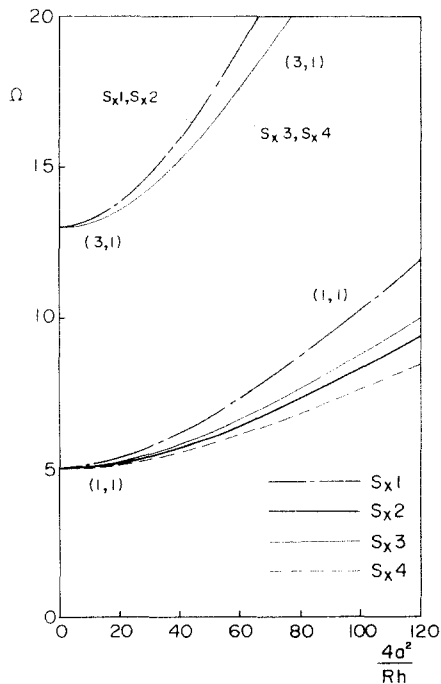


FIG. 4(a). Natural frequencies for $\lambda = 2.0$ with the set $S_{x,2}$ of the boundary conditions at $y = -b$ and b .

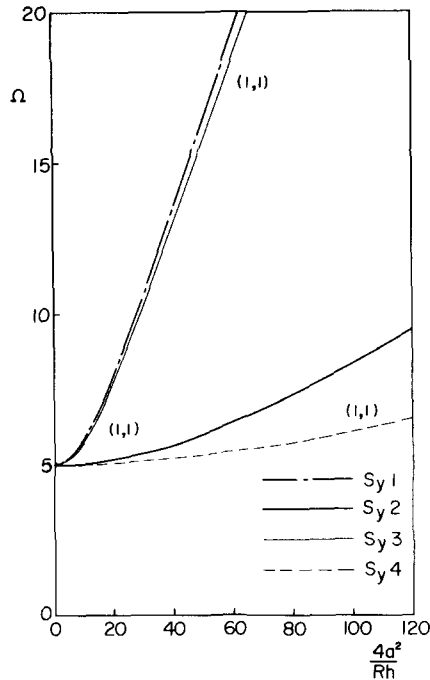


FIG. 4(b). Natural frequencies for $\lambda = 2.0$ with the set S_{x2} of the boundary conditions at $x = -a$ and a .

by the sets of S_{x1} , S_{x2} , S_{x3} and S_{x4} at $x = -a$ and a is presented by chain, solid, faint and dashed lines, respectively. When two lines can not be drawn separately, the one for the higher frequency is presented with an indication of both sets. The notation (p, q) indicates a natural mode predominated by an assumed mode of p and q half-waves in x and y directions, respectively.

It may be concluded from Figs. 2(a), 3(a) and 4(a) that the in-plane boundary conditions are quite influential to the natural frequency of the lower frequency mode, namely a $(1, 1)$ mode. In particular, the condition of zero tangential displacement v gives much restriction to a panel of aspect ratio $\lambda \lesssim 1$ compared with the condition of zero normal displacement u since the natural frequency for the case of the set S_{x1} or S_{x2} is much higher than for the case of the set S_{x3} or S_{x4} . Figure 4(a) indicates that for a higher value of aspect ratio the effect of the boundary conditions at $x = -a$ and a is diminished. The reason is that the distance between the edges at $x = -a$ and a relatively increases compared with the distance between the adjoining edges $y = -b$ and b as the aspect ratio increases.

It is noted that for a higher value of aspect ratio the condition of zero normal displacement u is more restrictive rather than that of zero tangential displacement v . The higher frequency mode, namely a $(3, 1)$ mode, is not so sensitive to the effect of the in-plane boundary conditions at $x = -a$ and a . The panel curvature has a large effect on the natural frequency of the lower and higher frequency modes.

Figures 2(b), 3(b) and 4(b) illustrate the influence of the in-plane boundary conditions at $y = -b$ and b with the combination of the set S_{x2} at $x = -a$ and a . In the figures the natural frequency of a panel constrained by the set S_{y1} , S_{y2} , S_{y3} or S_{y4} at $y = -b$ and b is indicated by a chain, a solid, a faint or a dashed line, respectively. Figures 2(b) and 3(b)

present typical illustrations that, except for the case of $S_{y,2}$, each natural mode is a combination of w_{11} and w_{13} , with the lower frequency mode being predominately w_{11} for small $4a^2/Rh$ and w_{13} for large $4a^2/Rh$. Conversely, the higher frequency mode is predominately w_{13} for small $4a^2/Rh$ and w_{11} for large $4a^2/Rh$.

It may be concluded from Figs. 2(b), 3(b) and 4(b) that the in-plane boundary conditions at $y = -b$ and b have a great influence on the natural frequency of the lower frequency mode. Especially the condition of zero normal displacement v is very restrictive to a panel since the natural frequency of a panel restrained by the set $S_{y,1}$ or $S_{y,3}$ is much higher than by the set $S_{y,2}$ or $S_{y,4}$. However, the influence decreases as the aspect ratio decreases. The boundary condition is less influential to the natural frequency of the higher frequency mode.

The summary of the numerical results is as follows: for a panel of aspect ratio $\lambda \gtrsim 1$ the conditions at the straight edges, $y = -b$ and b , are more influential than the conditions at the curved edges, $x = -a$ and a . In particular, the restriction on the normal displacement v at the straight edges raises the natural frequency of the lower frequency mode to a great extent. For a panel of aspect ratio $\lambda \lesssim 1$ the conditions at the curved edges are very influential. At the curved edges the condition of zero tangential displacement v gives more restrictions to a panel of aspect ratio $\lambda < 1.83$ rather than that of zero normal displacement u . As for the higher frequency mode the influence of the in-plane boundary condition is diminished.

Although in the present analysis the influence of the in-plane boundary conditions can be investigated solely with the combination of the set $S_{x,2}$ or $S_{y,2}$ at the adjoining edges, the combination of the different set from $S_{x,2}$ or $S_{y,2}$ might be expected to have a qualitatively similar influence on the natural frequency. The present approach based on Reissner's simplified equations for thin shallow shells has limitations on a range of panel curvature and on a choice for combination of sets of the in-plane boundary conditions. However, it provides a useful tool for estimation on the natural frequency of shallow curved panels including the effect of the in-plane boundary conditions.

In the Appendix is presented the derivation of the modal equations and the associated in-plane boundary conditions of shallow curved shells defined in the shell coordinate system shown in Fig. 5. It is also indicated that the natural frequency of thin cylindrical shells based on the Donnell type approximation is easily evaluated by utilizing the present analysis with appropriate modifications. Forsberg [11] has presented a range of shell geometry, for which the Donnell type approximation and omission of the in-plane inertia give accurate results.

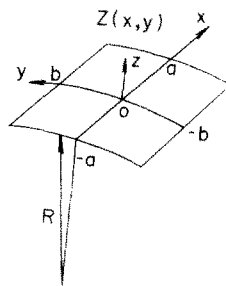


FIG. 5. Shell coordinates and shell geometry.

The present approach, in which a homogeneous solution of stress function is expressed in terms of trigonometric and hyperbolic functions in order to satisfy several combinations of the in-plane boundary conditions exactly, is also applicable to a nonlinear analysis of flexural vibration of rectangular plates [12].

The application of the present approach to panel flutter analysis of curved panels will be presented elsewhere.

4. CONCLUSIONS

The natural frequency of curved panels is evaluated on a basis of Reissner's simplified equations, which are approximately solved with the aid of Galerkin's method. The flexural vibration mode is assumed in a form of Fourier series and a homogeneous solution of stress function is expressed in terms of trigonometric and hyperbolic functions.

Numerical results indicate that the in-plane boundary conditions have a great influence on the natural frequency as well as the panel geometry. Although the present approach has limitations on a range of panel curvature and on a choice for combination of the in-plane boundary conditions, it provides a useful tool for estimation of the natural frequency of curved panels.

Acknowledgement—The author would like to express his appreciation to Associate Professor S. Kobayashi of the University of Tokyo for his valuable advices.

REFERENCES

- [1] V. Z. VLASOV, *General Theory of Shells and Its Applications in Engineering*, NASA TT F-99 (1964).
- [2] P. J. PALMER, The natural frequency of vibration of curved rectangular plates. *Aeronaut. Q.* **5**, 101 (1954).
- [3] E. REISSNER, On transverse vibrations of thin, shallow elastic shells, *Q. appl. Math.* **13** (2), 169 (1955).
- [4] K. MARGUERRE, Zur Theorie der gekrümmten Platte grosser Formänderung, *Proc. Fifth Inter. Cong. Appl. Mech.* pp. 93–101 (1938).
- [5] S. KOBAYASHI, *The Theory of Light Structures and Its Applications* (in Japanese), edited by T. HAYASHI, chapter 10. Nikkagiren (1966).
- [6] J. L. SEWALL, Vibration Analysis of Cylindrically Curved Panels with Simply Supported or Clamped Edges and Comparison with some Experiments, NASA TN D-3791 (1967).
- [7] J. J. WEBSTER, Free vibrations of rectangular curved panels. *Int. J. mech. Sci.* **10** (7), 571 (1968).
- [8] E. H. DOWELL, Nonlinear flutter of curved plates. *AIAA Jnl* **7** (3), 424 (1969).
- [9] K. FORSBERG, Influence of boundary conditions on the modal characteristics of thin cylindrical shells. *AIAA Jnl* **2** (12), 2150 (1964).
- [10] T. HAYASHI and K. KONDO, On the Buckling Loads and Postbuckling Behavior of Curved Panels under Axial Compression, *Proc. Eighth Int. Symp. Space Techn. Sci.*, Tokyo, pp. 259–268 (1969).
- [11] K. FORSBERG, A Review of Analytical Methods used to Determine the Modal Characteristics of Cylindrical Shells, NASA CR-613 (1966).
- [12] Y. MATSUZAKI, Influence of the In-Plane Boundary Conditions on the Nonlinear Characteristics of Flexural Vibration of Rectangular Plates, Presented at *12th Conf. Strength Struct.*, Japan Soc. Aero Space Sci. (1970).

APPENDIX

In the text of the paper the rectangular cartesian coordinate system shown in Fig. 1 is used for a shallow curved panel. For comparison the shell coordinate system shown in Fig. 5 will be employed here in order to obtain the modal equations and the associated in-plane boundary conditions. The definition of the breadth $2b$ along y direction and the direction

of the displacement v are different between both coordinate systems. However, the differences may be negligible for a shallow curved panel.

The strain displacement relations of the middle-surface of a panel are given in the shell coordinate system as

$$\begin{cases} \varepsilon_{x0} = \frac{\partial u}{\partial X} \\ \varepsilon_{y0} = \frac{\partial v}{\partial y} + \frac{w}{R} \\ \gamma_{xy0} = \frac{\partial u}{\partial y} + \frac{\partial v}{\partial X} \end{cases} \quad (\text{A1})$$

Since the conditions

$$\frac{\partial^2 Z}{\partial X^2} = 0, \quad \frac{\partial^2 Z}{\partial y^2} = -\frac{1}{R}, \quad \frac{\partial^2 Z}{\partial X \partial y} = 0 \quad (\text{A2})$$

are satisfied by equation (3), the equations of equilibrium and compatibility defined in the shell coordinate system are identical with equations (4) and (5), respectively. Equations (9) are used as an assumed mode of flexural vibration and hence equations (10) are obtained as a stress function. Consequently the expressions of stress resultants N_x , N_y and N_{xy} and the displacement u are identified with those given by equations (13)–(16). Therefore, if the expression of the displacement v proves to be identical with equations (17) while a vibration mode being symmetrical in y direction, the modal equations are the same as equations (19).

Partial integration of equation (17.1) and utilization of equation (A2) yield

$$v(y) = \frac{\partial Z}{\partial y} w_0 + \int_0^y \left[\frac{1}{Eh} (N_y - vN_x) + \frac{w}{R} \right] dy. \quad (17)^*$$

The integral in equation (17)* is identical with the expression of the displacement v defined in the shell coordinate system. Since the first term of the right-hand side of equation (17)* vanishes at $y = -b$ or b , equation (17)* becomes equivalent to the displacement v in the shell coordinate system at $y = -b$ and b .

As shown in the above, the modal equations defined in the shell coordinate system have formally the same expressions as those defined in the rectangular cartesian coordinate system. Therefore, the frequency defined in the shell coordinate system is identical with that defined in the rectangular cartesian coordinate system.

In addition, this fact implies that the natural frequency of a thin cylindrical shell calculated from a basis on the Donnell type approximation is easily evaluated by utilizing the present analysis for an antisymmetrical vibration mode in y direction with appropriate modifications. The value of a half of breadth should be πR in place of b . The condition of continuity at $y = -\pi R$ and πR is satisfied by using the set S_2 .

Абстракт—На основе упрощенных уравнений Рейсснера для тонких, пологих оболочек определяется собственная частота для панелей перекрытия. Уравнения решаются приблизительно с помощью метода Галеркина. Принимается вид изгибных колебаний в виде рядов Фурье.

Ищется однородное решение функций напряжений в форме тригонометрических и гиперболических функций, с целью точного удовлетворения некоторой системе граничных условий в плоскости. Уравнения колебаний вообще сопряжены и следовательно каждый вид собственных колебаний является общей комбинацией принятых видов колебаний. Численные результаты в аппроксимации двух видов колебаний указывают на то, что условия на прямых краях имеют большее влияние, чем условия на кривых краях для панели при $\lambda \geq 1$, где λ является отношением длины прямого края к длине кривого. В частности, ограничение нормальных перемещений на прямых краях повышает, в большой степени собственную частоту вида колебаний низкой частоты. Для $\lambda \leq 1$ условия на кривых краях очень влиятельны. На кривых краях условие нулевого тангенциального перемещения даёт больше ограничений для панели при $\lambda < 1,83$, чем условие нулевого нормального перемещения. Влияние граничных условий в плоскости уменьшается для видов колебаний высокой частоты.